0026-895X/06/6906-1905–1912
MOLECULAR PHARMACOLOGY
U.S. Government work not protected by U.S. copyright
Mol Pharmacol 69:1905–1912, 2006

Vol. 69, No. 6
20685/3113379
Printed in U.S.A.

The Two-State Dimer Receptor Model: A General Model for Receptor Dimers[S]

Rafael Franco, Vicent Casadó, Josefa Mallol, Carla Ferrada, Sergi Ferré, Kjell Fuxe, Antoni Cortés, Francisco Ciruela, Carmen Lluis, and Enric I. Canela

Department of Biochemistry and Molecular Biology, University of Barcelona, Barcelona, Spain (R.F., V.C., J.M., C.F., A.C., F.C., C.L., E.I.C.); National Institute on Drug Abuse, National Institutes of Health, Department of Health and Human Services, Baltimore, Maryland (S.F.); and Department of Neuroscience, Division of Cellular and Molecular Neurochemistry, Karolinska Institutet, Stockholm, Sweden (K.F.)

Received November 9, 2005; accepted February 23, 2006

ABSTRACT

Nonlinear Scatchard plots are often found for agonist binding to G-protein-coupled receptors. Because there is clear evidence of receptor dimerization, these nonlinear Scatchard plots can reflect cooperativity on agonist binding to the two binding sites in the dimer. According to this, the "two-state dimer receptor model" has been recently derived. In this article, the performance of the model has been analyzed in fitting data of agonist binding to A_1 adenosine receptors, which are an example of receptor displaying concave downward Scatchard plots. Analysis of agonist/antagonist competition data for dopamine D_1 receptors using the two-state dimer receptor model has also been performed. Although fitting to the two-state dimer receptor model was similar to the fitting to the "two-independent-site receptor model", the former is simpler, and a discrimination test selects the two-state dimer receptor model as the best. This model was also very robust in fitting data of estrogen binding to the estrogen receptor, for which Scatchard plots are concave upward. On the one hand, the model would predict the already demonstrated existence of estrogen receptor dimers. On the other hand, the model would predict that concave upward Scatchard plots reflect positive cooperativity, which can be neither predicted nor explained by assuming the existence of two different affinity states. In summary, the two-state dimer receptor model is good for fitting data of binding to dimeric receptors displaying either linear, concave upward, or concave downward Scatchard plots

In 1983, Fuxe et al. formulated the hypothesis about the existence of homodimers for different types of heptaspanning membrane receptors. In the same year, Avissar et al. (1983) published the first demonstration of G-protein-coupled receptor homodimers and homotetramers of muscarinic receptors. The authors suggested that the muscarinic receptor exists in oligomeric forms and that a dimer and tetramer may exist as interconvertible species. This was not seriously considered until 10 year later after the demonstration of further receptor homodimers in cells expressing recombinant receptors and in membranes from mammalian brain (Ng and George, 1994; Ciruela et al., 1995). Among others, D_1 and D_2 dopamine, A_1 and A_{2A} adenosine, muscarinic, peptide P, GABA, metabotropic glutamate, opioid, adrenergic, histamine, serotonin, and chemokine receptors can be found as homodimers in living cells (Bouvier, 2001; Milligan and White, 2001; Agnati et al., 2003; Bai, 2004; Urizar et al., 2005 and references therein). For A_{2A} adenosine receptors and probably for other receptors, dimers are the physiological species that is activated by the physiological ligand; thus, whereas monomers and dimers of A_{2A} adenosine receptors appear in living cells, the dimers are found predominantly on the cell surface (Canals et al., 2004). These data strongly suggest a key role of dimers in the nonlinear Scatchard plots found for ligand binding and in the mechanism of operation of heptaspanning receptors.

As occasionally speculated (Avissar el al., 1983; Wreggett and Wells, 1995; Lazareno et al., 1998; Trankle et al., 2003; Urizar at al., 2005), it is readily obvious that the available experimental evidence points out the impossibility of ex-

F.C. holds a Ramón y Cajal research contract with the Ministerio de Ciencia y Tecnología. This work was supported by grants SAF2002-03293 (to R.F.), SAF2005-00903 (to F.C.), and SAF2005-00170 (to E.I.C.) from Ministerio de Ciencia y Tecnología.

[S] The online version of this article (available at http://molpharm.aspetjournals.org) contains supplemental material.

Article, publication date, and citation information can be found at http://molpharm.aspetjournals.org.
doi:10.1124/mol.105.020685.

ABBREVIATIONS: (*R*)-PIA, (−)-N^6-(2-phenylisopropyl)adenosine; [^{3}H](*R*)-PIA, [^{3}H(G)](*R*)-PIA; SCH 23390, (*R*)-(+)-7-chloro-8-hydroxy-3-methyl-1-phenyl-2,3,4,5-tetrahydro-1*H*-3-benzazepine; [^{3}H]SCH 23390, [*N*-methyl-^{3}H]SCH 23390; SKF 38393, (±)-1-phenyl-2,3,4,5-tetrahydro-(1*H*)-3-benzazepine-7, 8-diol; A_1R, A_1 adenosine receptor.

plaining the operation of heptaspanning receptors without considering dimers as the minimum structure for many heptaspanning receptors. This evidence has led us to revisit the existing models to take into account dimers and to devise a novel model that includes dimers as basic units (Franco et al., 2005). This model, the "two-state dimer receptor model", considers a ligand-induced conformational change from one component of the dimer to be communicated to the other (Fig. 1). The two-state dimer receptor model is based on the communication between the two subunits of the receptor dimer. The model is an extension of the "two-state model of receptor activation" but considers dimeric structures able to bind one molecule to the orthosteric center in each monomer. Assuming receptor isomerization between inactive (R_2) and active (R_2*) species, the model is able to explain the behavior of heptaspanning membrane receptors. Negative or positive cooperativity is naturally explained by assuming that binding of the first ligand modifies the equilibrium parameters defining the binding of the second ligand molecule. Among other features, the two-state-dimer model predicts that cooperativity in the binding of all type of molecules to the orthosteric center would depend on the degree of constitutive activity (Franco et al., 2005). In this study, we tested the performance of the model using saturation binding and competition binding data for G-protein-coupled dimeric receptors and for dimeric receptors not coupled to G-proteins.

Materials and Methods

Membrane Preparation and Protein Determination. Membrane suspensions from lamb brain cortex or striatum were obtained as described previously (Casadó et al., 1990). Tissue was disrupted with a Polytron homogenizer (PTA 20 TS rotor, setting 3; Kinematica, Basel, Switzerland) for three 5-s periods in 10 volumes of 50 mM Tris-HCl buffer, pH 7.4. Tissue debris were separated by centrifugation (900*g*, 10 min, 4°C). Membranes were then obtained by centrifugation at 105,000*g* (40 min, 4°C), and the pellet was resuspended and recentrifuged under the same conditions. The pellet was stored at −80°C and was washed once more as described above and resuspended in 50 mM Tris-HCl buffer for immediate use. Protein was quantified by the bicinchoninic acid method (Pierce Chemical Co., Rockford, IL) using bovine serum albumin as standard.

Radioligand Binding Experiments. Membrane suspensions from lamb brain cortex or striatum (0.2–0.3 mg of protein/ml) were incubated with increasing radioligand concentrations: triplicates of 8 different concentrations, from 0.01 to 24 nM, of the A_1 adenosine receptor agonist [^{3}H](*R*)-PIA (30.5 Ci/mmol; Moravek Biochemicals Inc., Brea, CA) or from 0.09 to 10.5 nM of the D_1 dopamine receptor antagonist [^{3}H]SCH 23390 (85 Ci/mmol; PerkinElmer Life and Analytical Sciences, Boston, MA) at 25°C in 50 mM Tris-HCl buffer, pH 7.4, containing 10 mM $MgCl_2$ and for [^{3}H](*R*)-PIA binding, 0.2 U/ml adenosine deaminase (EC 3.5.4.4; Roche Diagnostics S.L., Sant Cugat del Vallès, Spain). After incubation time sufficient to achieve the equilibrium for the lowest radioligand concentration (5 h), free and membrane-bound radioligand were separated as described later. Nonspecific binding was defined as the binding remaining in the presence of 50 μM (*R*)-PIA (SigmaAldrich Chemical Co.) (Casadó et al., 1990), or 50 μM SCH 23390 (Tocris Cookson Ltd., Avonmouth, UK).

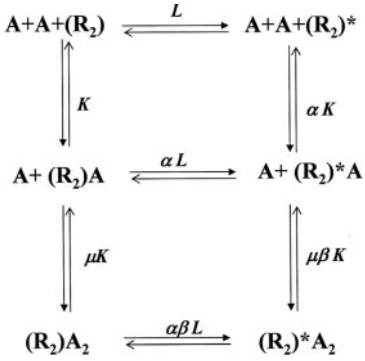

Fig. 1. Two-state dimer receptor model. *K* is the equilibrium association constant of A to R_2, *L* is the equilibrium receptor isomerization constant, α is the intrinsic efficacy of A binding to unoccupied receptors, β is the intrinsic efficacy of A binding to single-occupied receptor, and μ is the intrinsic association constant of A.

Competition experiments were performed by incubating (90 min) membranes from lamb brain striatum (0.3 mg of protein/ml) at 25°C in 50 mM Tris-HCl buffer, pH 7.4, containing 10 mM $MgCl_2$ and 0.2 U/ml adenosine deaminase with 1.2 nM [^{3}H]SCH 23390 in the absence or presence of increasing concentrations (triplicates of 12 different competitor concentrations from 0.1 nM to 50 μM) of nonlabeled D_1 dopamine receptor agonist SKF 38393 (Tocris Cookson Ltd., Avonmouth, UK). Nonspecific binding was determined in the presence of 50 μM SCH 23390.

In all cases, free and membrane-bound ligand were separated by rapid filtration of 500-μl aliquots in a cell harvester (Brandel, Gaithersburg, MD) through Whatman GF/C filters embedded in 0.3% polyethylenimine, which were subsequently washed for 5 s with 5 ml of ice-cold Tris-HCl buffer. The filters were incubated with 10 ml of Ecoscint H scintillation cocktail (National Diagnostics, Atlanta, GA) overnight at room temperature and radioactivity counts were determined using a Tri-Carb 1600 scintillation counter (PerkinElmer Life and Analytical Sciences) with an efficiency of 62% (Sarrió et al., 2000).

Data Analysis. The specific binding data from the saturation or competition experiments were all analyzed by nonlinear regression, using the commercial Grafit curve-fitting software (Erithacus Software, Staines, Middlesex, UK). This software consists of an iterative procedure based on the Marquardt algorithm. This procedure allows the use of two or more independent variables (e.g., time and concentration), which was necessary for the analyses reported in this article.

Results are given as parameter values ± S.E.M. and differences respect to controls have been tested for significance ($P < 0.05$) using Student's *t* test for unpaired samples. Goodness of fit was tested according to reduced χ^2 value given by the nonlinear regression program. The test of significance for two different model population variances was based upon the F-distribution (see Casadó et al., 1990 for details). Using this F-test, a probability greater than 95% ($P < 0.05$) was considered the criterion to select a more complex model over the simplest one. In all cases, a probability of less than 70% ($P > 0.30$) resulted when one model was not significantly better than the other.

Results

Saturation Binding Isotherms for Receptors Coupled to G-Proteins: Agonist Binding to A_1 Adenosine Receptors. The A_1 adenosine receptor (A_1R) is a prototypic example of a heptaspanning membrane receptor with apparently complex kinetics of agonist binding. The binding of different full agonists displays nonlinear biphasic Scatchard plots, indicating apparent negative cooperativity (Casadó et al., 1991; Franco et al., 1996). This corresponds to an equation of second-degree numerator and second-degree denominator (or 2:2 functions) and not to simple Michaelian functions (or 1:1 functions). To investigate the behavior of agonist binding to A_1R, the binding of increasing concentrations of the specific A_1R agonist, (*R*)-PIA, to brain cortical membranes was performed. The experimental data

(Fig. 2) were numerically analyzed using different 2:2 functions and, for comparison, using a 1:1 function. Data were also fitted to a classic "two-independent-state model" using the following equation

$$[A]_{Bound} = \frac{R_1[A]}{K_1 + [A]} + \frac{R_2[A]}{K_2 + [A]} \quad (1)$$

where K_1 and K_2 stand for the equilibrium dissociation constant for the high- and low-affinity states and R_1 and R_2 are the number of high- and low-affinity states. The parameter values are shown in Table 1.

Considering that A_1R forms homodimers (Ciruela et al., 1995), a more realistic model for this receptor is the two-state dimer receptor model shown in the Fig. 1. The functional A_1R unit is the homodimer, each monomer having a binding site for the agonist. Binding of agonists to these dimers is represented by the function:

$$[A]_{Bound} = \frac{K[A] \times (1 + \alpha L) + 2 \times K^2\mu[A]^2 \times (1 + \alpha\beta L)}{1 + L + K[A] \times (1 + \alpha L) + K^2\mu[A]^2 \times (1 + \alpha\beta L)} \cdot [R_T] \quad (2)$$

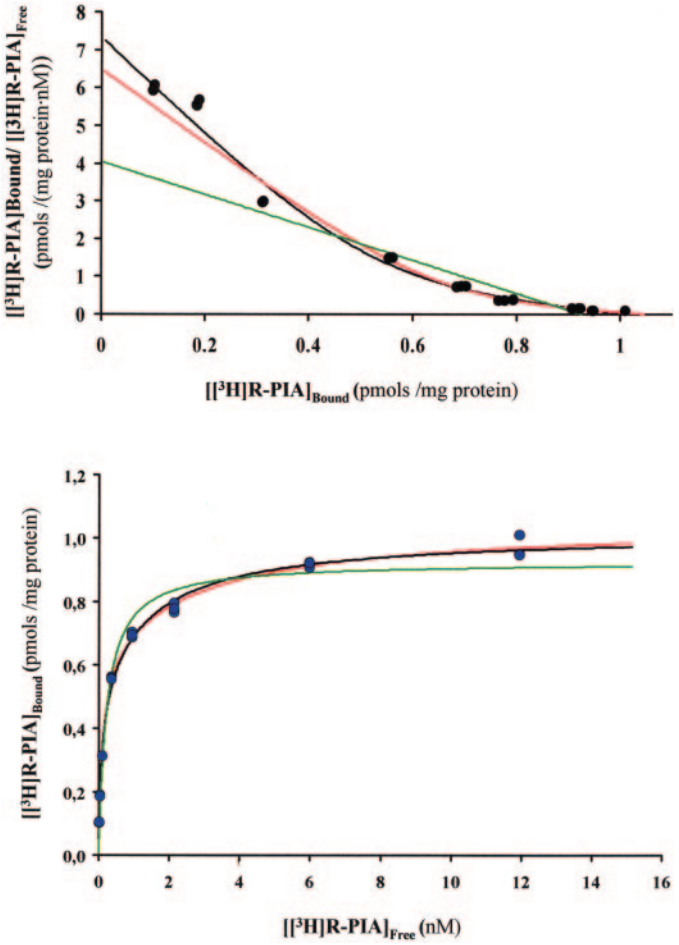

Fig. 2. Saturation curves (bottom) and Scatchard plot (top) for the agonist [^{3}H](R)-PIA binding to A_1 adenosine receptors from isolated lamb brain cortical membranes. The experiment was performed as described under *Materials and Methods*. Data were fitted according to the two-independent states receptor model (red), to the two-state dimer receptor model (black), and to a 1:1 function (green). The parameter values are indicated in Table 1.

As shown in Fig. 1, the homodimer can be in inactive form (R_2) or in active form (R_2*). L is the equilibrium constant for the isomerization of the receptor from R_2 to R_2*. R_2 and R_2* can reversibly bind two molecules of ligand (A), one to each receptor in the dimer. As defined previously (Franco et al., 2005), the affinity constants for the first and second binding of A to the inactive form are K and μK, respectively, where μ is the intrinsic association constant for the binding of A to the second receptor in R_2, αK and $\mu\beta K$ are the affinity constants for the first and second binding of A to the active form R_2*, and α and β reflect the intrinsic efficacy of the first and second molecule of A entering the dimer.

Because there are only three independent parameters, the ligand binding equation can be rewritten as follows:

$$[A]_{Bound} = \frac{c_1[A] + 2 \times [A]^2}{c_2 + c_1[A] + [A]^2} R_T \quad (3)$$

where c_1 and c_2 stand for:

$$c_1 = \frac{(1 + \alpha L)}{K \times \mu \times (1 + \alpha\beta L)}$$
$$c_2 = \frac{(1 + L)}{K^2\mu \times (1 + \alpha\beta L)} \quad (4)$$

Data from Fig. 2 were fitted to this equation, and R_T, c_1, and c_2 were determined. Values appear in Table 1. It should be noted that $c_2 = ([A]_{50})^2$ (i.e., the square of the semisaturation concentration). Thus, $\sqrt{c_2}$ gives information about the receptor affinity for the ligand. It is noteworthy that c_1 is related to cooperativity. $c_1 = 2 \times [A]_{50}$ denotes noncooperativity and, in this case, $c_2 = {c_1}^2/4$; therefore, the 2:2 binding isotherm simplifies to a 1:1 function. Values of $c_1 < 2 \times [A]_{50}$ indicate positive cooperativity; values of $c_1 > 2 \times [A]_{50}$ indicate negative cooperativity.

As shown in Fig. 2 and Table 1, an F-test demonstrates that the equations of two-independent-site receptor model and two-state dimer receptor model fit the data significantly better than the 1:1 equation. Because no improvement ($P >$ 0.30; probability of less than 70%) is obtained with one extra

TABLE 1

Parameter values obtained fitting the data of the agonist [^{3}H](R)-PIA binding to A_1 adenosine receptors, shown in Fig. 2, to different models

Nonspecific binding was determined in the presence of an excess of (R)-PIA as described in Saura et al. (1996). The determined value for nonspecific binding was 0.029 pmol/mg protein/nM. Data are presented as mean ± S.E.M. values given by the regression program (GRAFIT).

Parameter	Value
Two-state dimer receptor model[a]	
R_T[b]	0.509 ± 0.008 pmol/mg protein
c_1	1.42 ± 0.18 nM
c_2	0.098 ± 0.014 nM^2
$[A]_{50}$	0.313 nM
Models in Fig. 7 (1:1 equation)	
R_1	0.925 ± 0.019 pmol/mg protein
K_1	0.228 ± 0.023 nM
Two-independent-site receptor model[c]	
R_1	0.63 ± 0.05 pmol/mg protein
K_1	0.100 ± 0.014 nM
R_2	0.42 ± 0.04 pmol/mg protein
K_2	2.6 ± 0.9 nM

[a] $P < 0.05$ comparing models represented by a 1:1 equation and the two-state dimer receptor model.
[b] Maximum binding = $2 \times R_T$ = 1.018 pmol/mg protein.
[c] $P > 0.30$ comparing the classic "two-independent-site 1" and the two-state dimer receptor model.

parameter (two-independent-site receptor model), the simplest model explaining the experimental data for the binding of (*R*)-PIA to A_1 adenosine receptors is the two-state dimer receptor model. In addition, the fact that these receptors are dimers is a strong confirmation for the two-state dimer receptor model. In the two-state dimer receptor model, the value of $[A]_{50}$ yields information about the receptor affinity for (*R*)-PIA (0.313 nM). This parameter can be interpreted as the K_D in models assuming receptor monomers. An interesting aspect of this model is that fitting experimental data to the eq. 3 gives direct information about cooperativity. As can be observed in Table 1, the value of c_1 is 1.42 nM and is therefore significantly ($P < 0.01$) greater than $2 \times [A]_{50}$ (2×0.313), which is an indication of negative cooperativity. This would indicate that (*R*)-PIA binds to a dimeric receptor (R_2) giving the complex (R_2)–(*R*)-PIA, and that a second molecule of (*R*)-PIA binds to this complex with less affinity, then yielding the complex (*R*)-PIA–(R_2)–(*R*)-PIA. Both complexes would isomerize, giving the corresponding active forms.

Competition Experiments for Receptors Coupled to G-Proteins: Antagonist Binding to D_1 Dopamine Receptor. For some receptors, a saturation curve is not the best choice to analyze ligand binding behavior (i.e., in cases where ligands have low affinity or ligands are not available in radiolabeled form, competition experiments are useful to evaluate binding characteristics). The pharmacology of the D_1 dopamine receptor, a heptaspanning G-protein-coupled membrane receptor is usually analyzed by competition experiments. In this study, the affinity of the specific D_1 receptor agonist SKF 38393 was determined from competition assays using the specific antagonist [^{3}H]SCH 23390 as radioligand bound to brain striatal membranes.

Irrespective of the model considered, to deduce the binding parameters of a ligand acting as competitor, it is necessary to know in advance that the binding parameters of the radioligand. Thus, as described above for A_1 adenosine receptors, the saturation curve corresponding to the antagonist [^{3}H]SCH 23390 binding to D_1 receptors was first analyzed using the two-state dimer receptor model according to the eq. 3. Because c_2 was not significantly different from $2 \times [A]_{50}$ ($P > 0.30$), the antagonist binding to D_1 dopamine receptor is noncooperative. According to the data obtained by the two-state dimer receptor model, the Scatchard plot was linear, indicating noncooperativity or neutral cooperativity (Fig. 3). The values of R_T, $[A]_{50}$ and c_1 were deduced and appear in Table 2. It is easily deduced for noncooperativity that the ligand affinity ($[A]_{50}$) is $c_1/2$; therefore, the affinity of [^{3}H]SCH 23390 was estimated to be 0.78 nM.

An extension of the two-state dimer receptor model was used to fit the data of competition of antagonist, [^{3}H]SCH 23390, binding (A) with increasing concentrations of agonist SKF 38393 (B). The simultaneous antagonist and agonist binding to a dimeric receptor is now taken into account as indicated in Fig. 4. According to this scheme, the suitable equation to fit competition data deduced as indicated in Supplementary Material is

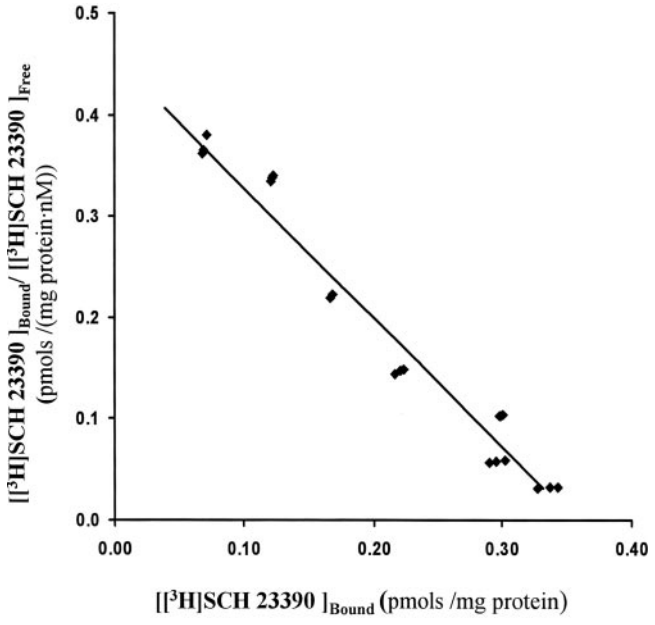

Fig. 3. Scatchard plot for the antagonist [^{3}H]SCH 23390 binding to D_1 dopamine receptors from isolated lamb brain striatal membranes. The experiment was performed as described under *Materials and Methods*. Data were fitted according to the two-state dimer receptor model. The parameter values are indicated in Table 2.

TABLE 2

Parameter values obtained fitting the data of the antagonist [^{3}H]SCH 23390 binding to D_1 dopamine receptors, shown in Fig. 3, to the two-state dimer receptor model

Nonspecific binding was determined in the presence of an excess of SCH 23390 as described under *Materials and Methods*. The determined value for nonspecific binding data was 0.039 pmol/mg protein/nM. Data are presented as mean ± S.E.M. values given by the regression program (GRAFIT).

Parameter	Value
R_T[a]	0.178 ± 0.003 pmol/mg protein
c_1	1.6 ± 0.1 nM
$[A]_{50}$	0.78 nM

[a] Maximum binding = $2 \times R_T$ = 0.356 pmol/mg protein.

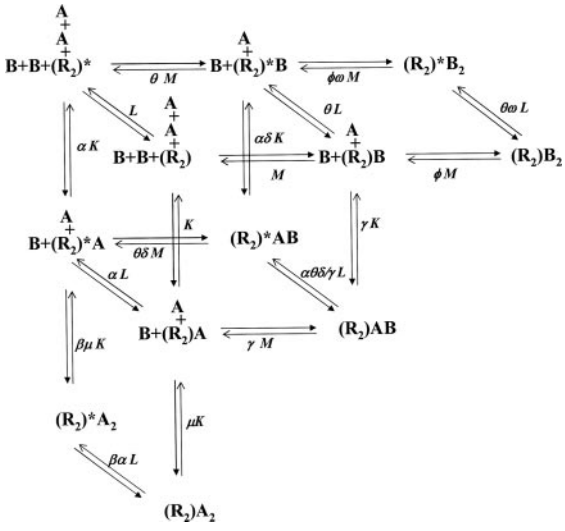

Fig. 4. Scheme of the two-state dimer receptor model when two ligands are used in competition assays. *K* is the equilibrium association constant of A to R_2, *L* is the equilibrium receptor isomerization constant, α is the intrinsic efficacy of A binding to unoccupied receptors, β is the intrinsic efficacy of A binding to single-occupied receptor, μ is the intrinsic association constant of A, and *M* is the equilibrium association constant of B to R_2. θ is the intrinsic efficacy of B binding to unoccupied receptors, ω is the intrinsic efficacy of B binding to single-occupied receptor, ϕ is the binding cooperativity between first and second B molecule: ratio of affinity of B for A(RR) and (RR); γ is the binding cooperativity between A and B: ratio of affinity of A for B(RR) and R or of B for A(RR) and RR, and δ is the activation cooperativity between A and B: ratio of affinity of A for B(RR)* and B(RR) or of B for A(RR)* and A(RR).

$$[A]_{Bound} = \frac{c_1[A] + 2 \times [A]^2 + c_5[A] \times [B]}{(c_2 + c_1[A] + [A]^2) + (c_3 + c_5[A]) \times [B] + c_4[B]^2} R_T \quad (5)$$

where c_1 to c_5 are a combination of constants (see Supplementary Material).

Fitting the experimental data (Fig. 5) to eq. 5 and taking into account that $c_2 = c_1^2/4$, $c_1 = 1.6$ nM (see Table 2) and that the concentration of the radioligand is 1.2 nM, the parameters deduced are indicated in Table 3. Values of c_3 and c_4 give information about affinity and cooperativity of agonist (B) binding to the receptor. Thus, the quotient c_2/c_4 corresponds to $([B]_{50})^2$ giving information about the affinity for the agonist ($[B]_{50}$). The value of 78 nM indicates a relatively low affinity of the agonist SKF 38393. Moreover the quotient c_3/c_4 is related to cooperativity: values of $c_3/c_4 = 2 \times [B]_{50}$ indicate noncooperativity, values of $c_3/c_4 < 2 \times [B]_{50}$ point out positive cooperativity, and values of $c_3/c_4 > 2 \times [B]_{50}$ indicate negative cooperativity. With the data provided in Table 3, $c_3/c_4 > 2 \times [B]_{50}$ (3300 versus 156 nM), which indicates that a strong negative cooperativity exists in the binding of SKF 38393 to D_1 receptors. The value of c_5 indicates the relative tendency to form the complex A(R_2)B with respect to that of forming A(R_2)A or B(R_2)B.

Saturation Curve for Receptors Not Coupled to G-Proteins: Agonist Binding to Estrogen Receptor. The dimer model was tested for radioligand binding to receptors that form dimers but are not coupled to G-proteins. The estrogen receptor is a convenient choice because binding of agonists show positive cooperativity (Fig. 6), which is rarely found for heptaspanning G-protein-coupled membrane receptors. Data of specific [^{3}H]estradiol binding to estrogen receptor from calf uteri, which was reported already in 1981 by Notides et al., is shown in Fig. 6. The two-independent-site receptor model is not suitable for this system because it cannot explain positive cooperativity. In this study, experimental data were examined using the two-state dimer receptor model. Data were fitted to eq. 3 and the parameters deduced are shown in Table 4. Because c_2 is the square of the semisaturation concentration, a value of $[A]_{50}$ of 0.642 nM is deduced that corresponds to the affinity of [^{3}H]estradiol for the estrogen receptor. More interestingly, c_1 denotes a strong positive cooperativity. In fact, the product $2 \times [Estrogen]_{50}$ is higher than c_1 (1.284 > 0.178), indicating positive cooperativity.

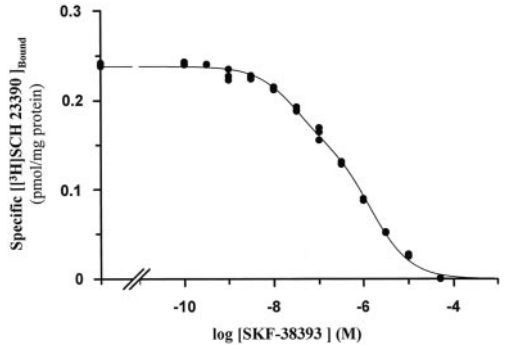

Fig. 5. Competition of 1.2 nM [^{3}H]SCH 23390 binding to lamb brain striatal D_1 dopamine receptors with SKF 38393. The experiment was performed as described under *Materials and Methods*. Data were fitted to the two-state dimer receptor model. The parameter values are indicated in Table 3.

Discussion

After the pioneering studies of receptor models devised by Colquhoun (1973) and Thron (1973), different models have been developed to describe the behavior of heptaspanning membrane receptors or G-protein coupled receptors (De Lean et al., 1980; Costa et al., 1992; Samama et al., 1993; Lefkowitz et al., 1993; Leff, 1995; Weiss et al., 1996a,b,c). Practically all published models are based on the "noncooperative mechanism" devised by del Castillo and Katz (1957) to explain the behavior of nicotinic acetylcholine receptors.

One of the most useful models so far is the two-state model of receptor activation, which assumes the occurrence of two different conformational states of the receptor molecule, R and R^* (Fig. 7a). In terms of signal transduction, the R form would be inactive, whereas the R^* form would be the active or productive form. These two conformational states, which are in equilibrium, have an orthosteric or "competitive" center for agonist binding. Filling this center shifts the equilibrium toward the productive form. On the other hand, there are synthetic compounds (which could be of pharmacological interest) that compete with the physiological agonist (i.e., they bind to the orthosteric center), leading to a variety of outputs, from full agonism/antagonism to partial/inverse agonism. The occurrence of equilibrium between the unproductive and the productive or active form may explain why some degree of signaling can happen in the absence of agonists, the so-called constitutive activity. Synthetic compounds that displace the equilibrium toward the inactive form upon binding to the

TABLE 3

Parameter values obtained by fitting the data of competition of the antagonist [^{3}H]SCH 23390 binding to D_1 dopamine receptors with SKF 38393, shown in Fig. 5, to the two-state dimer receptor model

Nonspecific binding was determined in the presence of an excess of SCH 23390 as described under *Materials and Methods*. The determined value for nonspecific binding was 0.039 pmol/mg protein/nM. Data are presented as mean ± S.E.M. values given by the regression program (GRAFIT).

Parameter	Value
R_T[a]	0.19 ± 0.01 pmol/mg protein
c_3	0.33 ± 0.03 nM
c_4	$(1.00 \pm 0.01) \times 10^{-4}$
c_5	0.0806 ± 0.015
$[B]_{50}$	78 nM
c_3/c_4	3300 nM

[a] Maximum binding = $2 \times R_T$ = 0.38 pmol/mg protein.

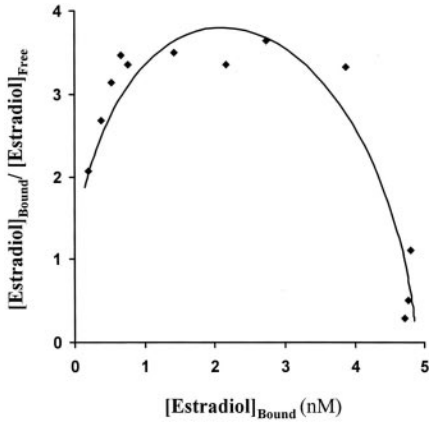

Fig. 6. Scatchard plot for the agonist estradiol binding to the estrogen receptor from calf uteri. Data were obtained from Notides et al. (1981). Data were fitted according to the two-state dimer receptor model. The parameter values are indicated in Table 4.

orthosteric center act as inverse agonists or negative antagonists by reducing the constitutive activity.

There are more complex models derived from the "ternary complex model" proposed by De Lean et al. (1980) (Fig. 7b), which, apart from the orthosteric center, includes an allosteric or regulatory site in which compounds not structurally related to agonists (e.g., G-proteins) can bind. The "ternary complex model of allosteric modulation" (Fig. 7c) is a modification of the ternary complex model (Fig. 7b) in which the allosteric modulation is not restricted to G-protein and includes different compounds that may have pharmacological activity acting on allosteric sites [see Lazareno et al. (1998) and references therein]. Samama et al. (1993) expanded this model and developed the "extended ternary complex model" (Fig. 7d), which included different affinity states (R and R^*) for the receptor uncoupled to G-protein. As in the two-state model, R is the unproductive form and R^* is the active form. In this model, the G-protein is assumed to bind to a specific and allosteric site in R^*. The G-protein, acting as an allosteric modulator, modifies the agonist binding and/or affects the equilibrium between R and R^*. Because the allosteric modulator, the G-protein in this case, does not compete with orthosteric compounds, maximum binding is not affected but K_D is. The "cubic ternary complex model" (Weiss et al., 1996a,b,c) (Fig. 7e) expands the extended ternary complex model, allowing the binding of G to R and R^*.

More recently the "allosteric two-state model" developed by Hall (2000) combines the ternary complex model of allosteric modulation (Fig. 7c) and the two-state model of receptor activation (Fig. 7a). This model (Fig. 7f), which is similar but more complex than the cubic ternary complex model, predicts the behavior of receptors when both orthosteric and allosteric compounds are present. More complex models, including the "quaternary complex model" of allosteric interactions, have been proposed assuming similar principles as those described above (Christopoulos and Kenakin, 2002).

Experimental data giving linear Scatchard plots were easily fitted to a single affinity state. However, the binding of agonists to heptaspanning receptors quite often give concave upward Scatchard plots. The above models do not explain suitably this behavior because they predict linear Scatchard plots for agonist binding to the orthosteric site. Concave upward Scatchard plots would be explained considering the existence of two separated (noninterconvertible forms) of the receptor: a high affinity form (R^* or G-protein coupled) and a low affinity form (R or G-protein uncoupled). The above-described models are based on an equilibrium between R and R^*; therefore, they would explain only nonlinear Scatchard plots if the concentration of G-protein is lower or similar than that of the receptor, something that does not occur under physiological conditions (Neubig, 1994). Moreover, it has been observed that the agonist induces changes in the proportions of the so called "high" and "low" affinity states, which strongly suggests that these two states cannot exist separately but are interconnected (Wong et al., 1986), and this apparent interconversion between states is independent of the G-protein (Casadó et al., 1991). Working with adenosine A_1 receptors, we showed that a full agonist led to an apparent change in the proportion of receptor in high and low affinity (Casadó et al., 1991). If the agonist is able to vary the proportion of high and low affinity states, these two forms would be in equilibrium, and consequently the two-independent-site receptor model cannot accurately represent the behavior of the receptors if the Scatchard plot is nonlinear.

Taking this into account, we claim that this type of nonlinear Scatchard plot is a consequence of negative cooperativity in the binding. Furthermore, concave downward Scatchard plots have been reported for agonist binding to muscarinic receptors (Lazareno et al., 1998), for agonist binding to μ- and δ-opioid receptors (Tomassini et al., 2003), and for agonist binding to H_2 and H_3 histamine receptors (Sinkins and Wells, 1993). In these cases, the reported models cannot explain Scatchard plots that probably reflect positive cooperativity.

We have postulated that to fully explain receptor behavior in terms of both ligand binding and receptor activation, both intramolecular and intermolecular interactions should be relevant (Franco et al., 2003). Ten years ago, heptaspanning receptors were believed to be composed of monomeric molecules. We proposed a model of heptaspanning receptor operation based on intermolecular receptor-receptor, receptor-protein, and receptor-lipid interactions. The "cluster-arranged cooperative model" (Franco et al., 1996) was the first formulated model able to explain nonlinear Scatchard plots for agonist binding to heptaspanning receptors on the basis of

TABLE 4

Parameter values obtained fitting the data of the agonist estradiol binding to the estrogen receptors, shown in Fig. 6, to the two-state dimer receptor model

Data were obtained from Fig. 2 in Notides et al. (1981). Data are presented as mean ± S.E.M. values given by the regression program (GRAFIT).

Parameter	Value
R_T[a]	2.44 ± 0.05 pmol/mg protein
C_1	0.178 ± 0.010 nM
C_2	0.42 ± 0.04 nM[2]
$[A]_{50}$	0.642 nM

[a] Maximum binding = 2 × R_T = 4.89 pmol/mg protein.

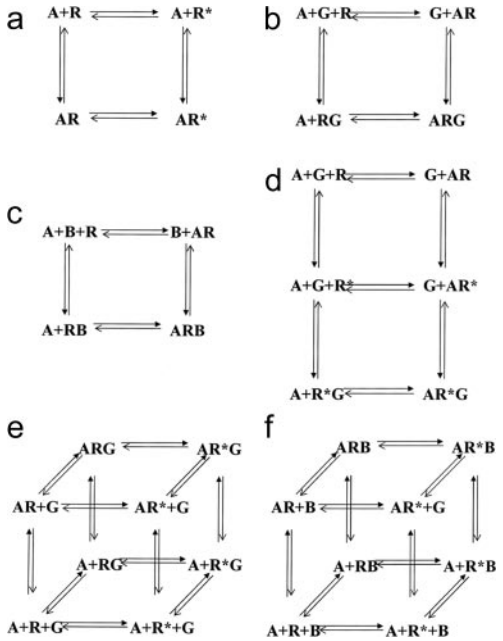

Fig. 7. Models for heptaspanning membrane receptor function. a, two-state model of receptor activation. b, the ternary complex model. c, the ternary complex model of allosteric modulation. d, the extended ternary complex model. e, the cubic ternary complex model. f, the allosteric two-state model.

negative cooperativity. We were aware of the requirement for receptor-protein and receptor-lipid interactions to achieve the conformational changes to be transmitted to the different receptor molecules and that would account for both negative and positive cooperativity. To explain the behavior of A_1 adenosine receptor, two extreme conformational states were assumed that correspond to high- and low-affinity binding states. In addition, the existence of a number of infinite conformational states with intermediate affinities was assumed. All of these forms would be in an equilibrium that would be affected by the agonist. According to the apparent negative cooperativity in the ligand binding and to the fact that agonist is able to cluster the receptors, it was assumed that receptors within the cluster (or microdomain) display a decreased affinity. A relevant feature in this model is the assumption that each agonist molecule that binds to the receptor is able to infinitesimally modify the affinity of subsequent agonist molecules interacting with the "empty" receptors in the cluster. This agonist-induced global change in the affinity is able to explain the negative cooperativity in the binding of adenosine to A_1 receptors (Franco et al., 1996).

A model consisting of a receptor molecule with more than one orthosteric site would also be able to explain cooperativity (positive, neutral, and negative). A receptor with more than one orthosteric site could be a monomer able to bind more than one agonist molecule or an oligomeric molecule having in each monomer one binding site (Franco et al., 1996; Franco et al., 2003). In this study, the binding of an agonist, (*R*)-PIA, to A_1 adenosine receptor has been analyzed using the two-state dimer receptor model, and the results have demonstrated that this is a suitable method for analyzing binding of radioligands to G-protein-coupled receptors showing cooperativity or not. Fitting the experimental data to a relatively simple equation (eq. 3), the parameters of ligand affinity and receptor cooperativity are easily deduced, thus characterizing the receptor behavior. The deduced parameter estimates agree with those obtained using the classic two-independent-site receptor model. Data from competition assays can also be fitted using the equations derived from the two-state dimer receptor model (eq. 5). It is demonstrated that the competition by an agonist (whose binding to the receptor shows cooperativity) of an antagonist binding to dopamine D_1 receptors has been well solved by the model and can be generalized to other dimeric receptors. Although the estrogen receptor is not coupled to G-proteins, it is a dimer of identical, interacting subunits (Bond et al., 1992), and estradiol binding to the receptor presents positive cooperativity. In cases like this, the classic models are not suitable to deduce the binding parameters because they cannot explain positive cooperativity. Data of estrogen binding is well fitted using the two-state dimer receptor model, allowing calculating ligand affinity and the degree of positive cooperativity using eq. 3. Thus, the two-state dimer receptor model is reliable for studying not only heptaspanning G-protein-coupled membrane receptors forming dimers but also other receptors capable of forming dimeric structures.

In conclusion, eqs. 3 and 5, derived from the two-state dimer receptor model, are simple equations to fit saturation experiments or competition experiments to obtain information about ligand affinity and cooperativity for dimeric receptors.

References

Agnati LF, Ferre S, Lluis C, Franco R, and Fuxe K (2003) Molecular mechanisms and therapeutical implications of intramembrane receptor/receptor interactions among heptahelical receptors with examples from the striatopallidal GABA neurons. *Pharmacol Rev* **55:**509–550.

Avissar S, Amitai G, and Sokolovsky M (1983) Oligomeric structure of muscarinic receptors is shown by photoaffinity labeling: subunit assembly may explain high- and low-affinity agonist states. *Proc Natl Acad Sci USA* **80:**156–159.

Bai M (2004) Dimerization of G-protein-coupled receptors: roles in signal transduction. *Cell Signal* **16:**175–186.

Bond JP, Sasson S, and Notides AC (1992) The binding of estrogen and estrogen antagonists to the estrogen receptor. *Arch Biochem Biophys* **296:**583–591.

Bouvier M (2001) Oligomerization of G-protein-coupled transmitter receptors. *Nat Rev Neurosci* **2:**274–286.

Canals M, Burgueño J, Marcellino D, Cabello N, Canela EI, Mallol J, Agnati L, Ferre S, Bouvier M, Fuxe K, et al. (2004) Homodimerization of adenosine A_{2A} receptors: qualitative and quantitative assessment by fluorescence and bioluminescence energy transfer. *J Neurochem* **88:**726–734.

Casadó V, Cantí C, Mallol J, Canela EI, Lluís C, and Franco R (1990) Solubilization of A_1 adenosine receptor from pig brain: characterization and evidence of the role of the cell membrane on the coexistence of high and low affinity status. *J Neurosci Res* **26:**461–473.

Casadó V, Mallol J, Canela EI, Lluis C, and Franco R (1991) The binding of [^{3}H]R-PIA to A_1 adenosine receptors produces a conversion of the high- to the low-affinity state. *FEBS Lett* **286:**221–224.

Christopoulos A and Kenakin T (2002) G protein-coupled receptor allosterism and complexing. *Pharmacol Rev* **54:**323–374.

Ciruela F, Casadó V, Mallol J, Canela EI, Lluis C, and Franco R (1995) Immunological identification of A_1 adenosine receptors in brain cortex. *J Neurosci Res* **42:**818–828.

Colquhoun D (1973) The relationship between classical and cooperative models for drug action, in *A Symposium on Drug Receptors* (Rang HP ed) pp 149–182, University Park Press, Baltimore.

Costa T, Ogino Y, Munson PJ, Onaran HO, and Rodbard D (1992) Drug efficacy at guanine nucleotide-binding regulatory protein-linked receptors: thermodynamic interpretation of negative antagonism and of receptor activity in the absence of ligand. *Mol Pharmacol* **41:**549–560.

De Lean A, Stadel JM, and Lefkowitz RJ (1980) A ternary complex model explains the agonist-specific binding properties of the adenylate cyclase-coupled b-adrenergic receptor. *J Biol Chem* **255:**7108–7117.

del Castillo J and Katz B (1957) A comparison of acetylcholine and stable depolarizing agents. *Proc R Soc Lond B Biol Sci* **146:**362–368.

Franco R, Canals M, Marcellino D, Ferre S, Agnati L, Mallol J, Casadó V, Ciruela F, Fuxe K, Lluis C, et al. (2003) Regulation of heptaspanning-membrane-receptor function by dimerization and clustering. *Trends Biochem Sci* **28:**238–243.

Franco R, Casadó V, Ciruela F, Mallol J, Lluis C, and Canela EI (1996) The cluster-arranged cooperative model: a model that accounts for the kinetics of binding to A_1 adenosine receptors. *Biochemistry* **35:**3007–3015.

Franco R, Casadó V, Mallol J, Ferré S, Fuxe K, Cortés A, Ciruela F, Lluis C, and Canela EI (2005) Dimer-based model for heptaspanning membrane receptors. *Trends Biochem Sci* **30:**260–366.

Fuxe K, Agnati LF, Benfenati F, Celani M, Zini I, Zoli M, and Mutt V (1983) Evidence for the existence of receptor-receptor interactions in the central nervous system. Studies on the regulation of monoamine receptors by neuropeptides. *J Neural Transm Suppl* **18:**165–179.

Hall DA (2000) Modeling the functional effects of allosteric modulators at pharmacological receptors: an extension of the two-state model of receptor activation. *Mol Pharmacol* **58:**1412–1423.

Lazareno S, Gharagozloo P, Kuonen D, Popham A, and Birdsall NJ (1998) Subtype-selective positive cooperative interactions between brucine analogues and acetylcholine at muscarinic receptors: radioligand binding studies. *Mol Pharmacol* **53:**573–589.

Leff P (1995) The two-state model of receptor activation. *Trends Pharmacol Sci* **16:**89–97.

Lefkowitz RJ, Cotecchia S, Samama P, and Costa T (1993) Constitutive activity of receptors coupled to guanine nucleotide regulatory proteins. *Trends Pharmacol Sci* **14:**303–307.

Milligan G and White JH (2001) Protein-protein interactions at G-protein-coupled receptors. *Trends Pharmacol Sci* **22:**513–518.

Neubig RR (1994) Membrane organization in G-protein mechanisms. *FASEB J* **8:**939–946.

Ng GY and George SR (1994) Dopamine receptor agonist reduces ethanol self-administration in the ethanol-preferring C57BL/6J inbred mouse. *Eur J Pharmacol* **15:**365–374.

Notides AC, Lerner N, and Hamilton DL (1981) Positive cooperativity of the estrogen receptor. *Proc Natl Acad Sci USA* **78:**4926–4930.

Samama P, Cotecchia S, Costa T, and Lefkowitz RJ (1993) A mutation-induced activated state of the b_2-adrenergic receptor. Extending the ternary complex model. *J Biol Chem* **268:**4625–4636.

Sarrió S, Casadó V, Escriche M, Ciruela F, Mallol J, Canela EI, Lluis C, and Franco R (2000) The heat shock cognate protein hsc73 assembles with A_1 adenosine receptors to form functional modules in the cell membrane. *Mol Cell Biol* **20:**5164–5174.

Saura C, Ciruela F, Casadó V, Canela EI, Mallol J, Lluis C, and Franco R (1996) Adenosine deaminase interacts with A_1 adenosine receptors in pig brain cortical membranes. *J Neurochem* **66:**1675–1682.

Sinkins WG and Wells JW (1993) G protein-linked receptors labeled by [^{3}H]histamine in guinea pig cerebral cortex. II. Mechanistic basis for multiple states of affinity [published erratum appears in *Mol Pharmacol* **44:**1278] *Mol Pharmacol* **43:**583–594.

Thron CD (1973) On the analysis of pharmacological experiments in terms of an allosteric receptor model. *Mol Pharmacol* **9:**1–9.
Tomassini N, Renaud FL, Roy S, and Loh HH (2003) Mu and delta receptors mediate morphine effects on phagocytosis by murine peritoneal macrophages. *J Neuroimmunol* **136:**9–16.
Trankle C, Weyand O, Voigtlander U, Mynett A, Lazareno S, Birdsall NJ, and Mohr K (2003) Interactions of orthosteric and allosteric ligands with [^{3}H]dimethyl-W84 at the common allosteric site of muscarinic M_2 receptors. *Mol Pharmacol* **64:**180–190.
Urizar E, Montanelli L, Loy T, Bonomi M, Swillens S, Gales C, Bouvier M, Smits G, Vassart G, and Costagliola S (2005) Glycoprotein hormone receptors: link between receptor homodimerization and negative cooperativity. *EMBO (Eur Mol Biol Organ) J* **24:**1954–1964.
Vilardaga JP, Bunemann M, Cárcel C, Castro M, and Lohse MJ (2003) Measurement of the millisecond activation switch of G protein-coupled receptors in living cells. *Nat Biotechnol* **21:**807–812.
Weiss JM, Morgan PH, Lutz MW, and Kenakin TP (1996a) The cubic ternary complex receptor-occupancy model I. Model description. *J Theor Biol* **178:**151–167.
Weiss JM, Morgan PH, Lutz MW, and Kenakin TP (1996b) The cubic ternary complex receptor-occupancy model II. Understanding apparent affinity. *J Theor Biol* **178:**169–182.
Weiss JM, Morgan PH, Lutz MW, and Kenakin TP (1996c) The cubic ternary complex receptor-occupancy model III. Resurrecting efficacy. *J Theor Biol* **181:**381–397.
Wong HM, Sole MJ, and Wells JW (1986) Assessment of mechanistic proposals for the binding of agonists to cardiac muscarinic receptors. *Biochemistry* **25:**6995–7008.
Wreggett KA and Wells JW (1995) Cooperativity manifest in the binding properties of purified cardiac muscarinic receptors. *J Biol Chem* **270:**22488–22499.

Address correspondence to: Rafael Franco, Dept. Bioquimica i Biologia Molecular, Universitat de Barcelona, Av. Diagonal, 645, 08028 Barcelona, Spain. E-mail: rfranco@ub.edu